RECENT IMPROVEMENTS TO A COMBINED NAVIER -STOKES FULL POTENTIAL METHODOLOGY FOR MODELING HORIZONTAL AXIS WIND TURBINES

SARUN BENJANIRAT, LAKSHMI N. SANKAR

sarun_benjanirat@ae.gatech.edu, lsankar@ae.gatech.edu
School of Aerospace Engineering
Georgia Institute of Technology
Atlanta, GA 30332-0150

ABSTRACT

A numerical technique has been developed for efficiently simulating fully three-dimensional viscous fluid flow around horizontal axis wind turbines (HAWT). In this approach, the viscous region surrounding the blades is modeled using 3-D unsteady Navier-Stokes equations. The inviscid region away from the boundary layer and the wake is modeled using potential flow. The concentrated vortices that emanate from the blade tip are treated as piecewise straight line segments that are allowed to deform and convect at the local flow velocity. Biot-Savart law is used to account for the velocity field associated with these vortices. This approach has been validated in the past for several HAWT configurations for which field and wind tunnel data are available.

In this study, we investigate the role that is played by inboard vortices, including the root vortex, on the HAWT aerodynamics and on the wind turbine performance. We investigate whether it is acceptable to neglect these effects, and model only the effects of the tip vortex. We also extend the hybrid approach to higher wind speeds where extensive separation is present. The effects of turbulence models on the calculations have also been studied. Comparisons with full Navier-Stokes simulations are also given.

INTRODUCTION

During the past decade, there has been an increased reliance on the use of computational methods to model and design horizontal axis wind turbines (HAWT). Many of the rotors found on current generation HAWT systems are designed using a combination of 2-D airfoil tools (Tangler[1], Eppler[2], and Selig[3]) and combined blade element and momentum theory (Glauert[4], Hansen,[5] Laino[6]). A number of comprehensive computer codes using this methodology are currently available. In these methods, unsteady flow effects are accounted for using unsteady potential flow theory and dynamic stall models (e.g. Leishman and Beddoes[7]). While computationally efficient and highly useful, these methods are incapable of accurately modeling three-dimensional cross flows, tower shadow effects, tip relief effects, and sweep effects. These three-dimensional effects can alter the airloads, affect the fatigue life, and significantly influence the total cost of ownership of HAWT systems.

First-principles-based modeling of these effects using Navier-Stokes solvers have been attempted by a number of researchers. These simulations can capture much of the physics in great detail. Full Navier-Stokes simulations of HAWT configurations have been done by scientists at NASA Ames (Earl Duque[8]) and in Denmark (Sorensen[9]). Sorensen, Michelsen and Schreck[10] have reported Navier-Stokes simulations for the NREL Phase VI rotor tested at NASA Ames Research Center. Madsen, Sorensen and Schreck[11] studied the effects of yaw on airloads. Duque, Burklund and Johnson[12] used the Navier-Stoke equations to model the NREL Phase VI rotor. Benjanirat, Sankar, and Xu[13] have studied effects of using k-ε model on the Navier-Stokes predictions.

OVERVIEW OF THE HYBRID METHOD

The high computational cost of detailed Navier-Stokes simulations limits their use in exploratory studies and design. To address the need for more efficient approaches, a combined Navier-Stokes/full potential equations based methodology has been developed by the present researchers. In this approach, the flow field is viewed as a combination of viscous regions, inviscid regions, and vortices as shown in Figure 1. These regions are modeled using different methodologies, making the present approach a hybrid method.

While the hybrid method shares some conceptual similarities with the classical viscous inviscid interaction analyses, it does not have any of the limitations of these methods. For example, the present method can be applied to 3-D unsteady viscous flows.

Conventional viscous-inviscid interaction methods are, for the most part, limited to steady flows. The present method has no singularities at the separation line, whereas the classical boundary-layer based interaction schemes have a strong mathematical singularity near separation.

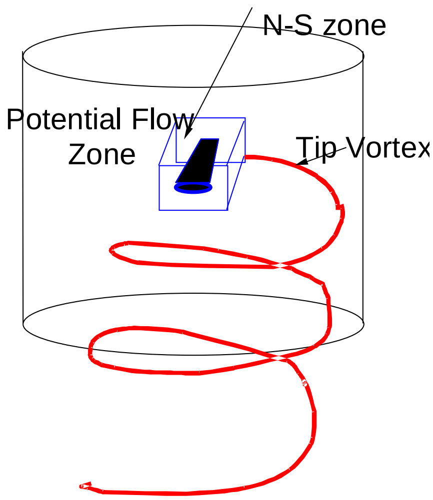

Figure 1. The Hybrid Methodology

This method has been extensively documented in several papers including the Ph. D dissertation and publications of Xu.[14-17]

IMPROVEMENTS TO THE HYBRID METHOD

The hybrid method has already been applied to the NREL Phase VI rotor at low wind speeds and encouraging results have been obtained. Because the size of the viscous region (Navier-Stokes zone) was kept very small in these studies (of the order of one chord length surrounding the blade), only flows at low wind speeds could be modeled. At higher wind speeds, where extensive separation was present, it was necessary to use a full Navier-Stokes solver.[13] Also, some of the elements of the flow such as the inboard (root) vortex were neglected once the vortex leaves the viscous flow region. Finally, many the earlier calculations with the hybrid method used a zero equation Baldwin-Lomax model or a one-equation Spalart-Allmaras model that have been validated only for attached or mildly separated flows.

In this work, we attempt to remove the limitations of the hybrid approach. We first study the effects of the root vortex. We next extend the speed range over which the hybrid method can be applied, essentially by enlarging the size of the Navier-Stokes zone to a distance of the order of one rotor radius surrounding the blade. We also investigate used of a two equation k-ε model. This model forms the basis for a more advanced 2-equation model such as k-ω model and its SST version, to be investigated in the future. The details of these improvements are briefly described below.

1. Modeling of the Effects of the Inboard Vortex

The original Hybrid methodology only models the vortex shed from the tip of the turbine blade using vortex markers. The root vortex is captured only in the Navier-Stokes zone, but is discarded in the full potential zone. The effect of neglecting the root vortices outside the Navier-Stokes zone is being studied in the present study by including the root vortex in a manner identical to the way the tip vortex is modeled.

2. Extension of the Hybrid Method to Higher Wind Speeds

The hybrid methodology was extended to higher wind speeds by enlarging the inner region so that much of the separated flow is captured using Navier-Stokes equations. While this increases the computer time somewhat, it is still more economical than a full Navier-Stokes approach.

To further improve the capability of the hybrid method to model massively separated flows, we also looked at replacing the zero and one-equation models present in the code with the following version of the k-ε model. The turbulent viscosity can be evaluated in terms of the turbulent kinetic energy k and the dissipation rate ε as follows:

$$\nu_T = \frac{C_\mu k^2}{\varepsilon}$$

The temporal and spatial evolution of k and ε was obtained from solving the following two equations using an alternating direction implicit time marching scheme.

Turbulent kinetic energy transport equation:

$$\frac{\partial k}{\partial t} + U_j \frac{\partial k}{\partial x_j} = \tau_{ij} \frac{\partial U_i}{\partial x_j} - \varepsilon + \frac{\partial}{\partial x_j}\left[(\nu + \frac{\nu_T}{\sigma_k}) \frac{\partial k}{\partial x_j} \right]$$

Where U_i is the time-averaged mean flow vector, τ_{ij} is the shear stress tensor and S_{ij} is the strain rate tensor.

Dissipation rate transport equation:

$$\frac{\partial \varepsilon}{\partial t} + U_j \frac{\partial \varepsilon}{\partial x_j} = C_{\varepsilon 1} \frac{\varepsilon}{k} \tau_{ij} \frac{\partial U_i}{\partial x_j} - C_{\varepsilon 2} \frac{\varepsilon^2}{k} + \frac{\partial}{\partial x_j}\left[(\nu + \frac{\nu_T}{\sigma_\varepsilon}) \frac{\partial \varepsilon}{\partial x_j} \right]$$

The constants in the k-ε formulation are listed below.

$$C_{\varepsilon 1} = 1.44, \ C_{\varepsilon 2} = 1.92, \ C_\mu = 0.09, \ \sigma_k = 1.0, \ \sigma_\varepsilon = 1.3$$

These are the “classical” constants, and no attempts have been made to modify them to improve the correlation.

The k-ε model can not reliably be used close to the surface area. This difficulty was addressed using a modification proposed by Gorski[18]. In this model, near the wall ε is assumed to be a constant in the inertial sub-layer, and k is assumed to be proportional to y^2 where y is the distance normal to the wall. This model has been independently evaluated by Wu, Huff and …kar[19] for oscillating airfoils and has been found to …atisfactory results.

…SULTS AND DISCUSSIONS

…culations reported in this study were …id. The flow field was divided into …bove the rotor disk and the other …nly one of the blades (called the …

…as “seen” by the reference …and tip vortex structures, … reference blade only …rom these vortex …38 points in the … the blade), 54 …ial locatio… …on n…

The hybrid calculations require 7 seconds per time step on single processor Pentium 4 class machine (2.6 GHz clock speed) while the Navier-Stokes calculations required 10 seconds per time step at high wind speeds. Hybrid and Navier-Stokes calculations both start with an initial representation of induced velocity field computed using Biot-Savart law, with the tip vortex geometry and strengths estimated from combined blade element momentum theory. Because this starting condition is a good representation of the flow field, the calculations converge quickly to a steady state, should one exist, within one revolution of the blade, as shown in figure 2. The convergence behavior is comparable to that of the Navier-Stokes analysis, indicating that the hybrid methodology retains most of the important physical phenomena that is modeled in a full Navier-Stokes analysis.

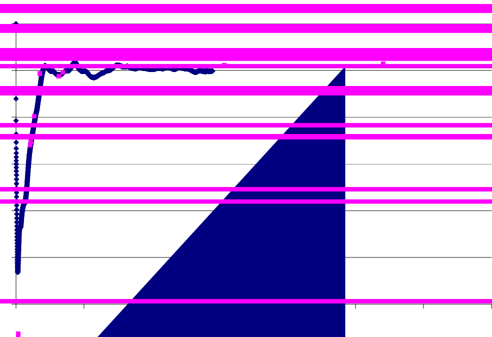

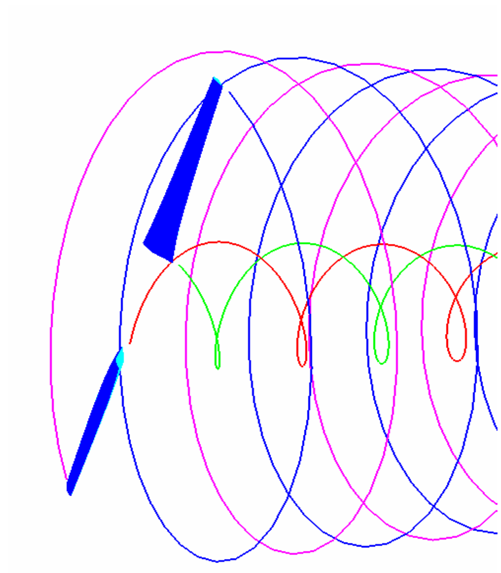

Figure 3. Geometry of Tip and Root Vortices for the Phase VI Rotor at 7m/s Wind

Table 1 show the low speed shaft torque modeled using the hybrid methodology with and without root vortex, compared with the NREL wind tunnel measurements. Our calculations indicate that the root vortex has little effect on the total torque. However, the root vortex does have a substantial effect on the angle of attack that the inboard sections see. The angle of attack tends to decrease at the root when that root vortex is included, leading to a somewhat smaller separation zone, as seen in figures 4a and 4b. A significant amount of centrifugal pumping of the low momentum fluid in the separated flow inboard is seen in figure 4.

Wind Speed (m/s)	NREL Measurements	Without the root vortex	With the root vortex
7	801.2651	705.2228	706.0739
10	1341.1022	1239.120	1246.1038

Table 1. Low Speed Shaft Torque for the Phase VI Rotor with and without Root Vortices, in Newton-meters

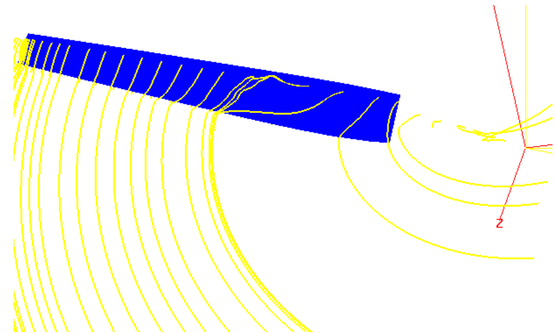

Figure 4a Calculated Flow Field without Root Vortex Markers for the Phase VI Rotor at 10m/s, indicating that a large separation zone at the root is present.

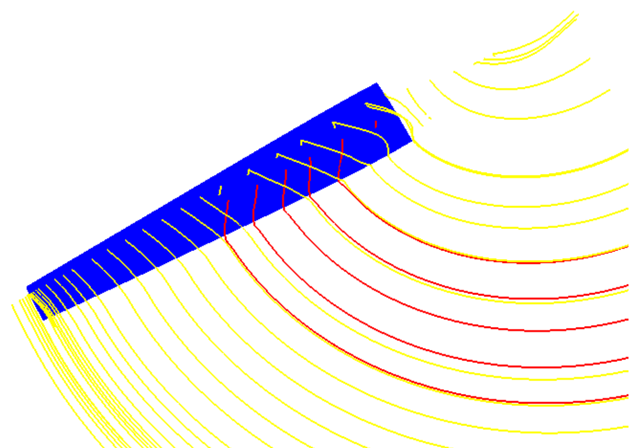

Figure 4b Calculated Flow Field with Root Vortex Markers for the Phase VI Rotor at 10m/s. A smaller separation region is present, and centrifugal pumping is observed.

BEHAVIOR OF THE HYBRID METHOD AT HIGHER WIND SPEEDS

As discussed earlier, the hybrid method has been extended to higher wind speeds by enlarging the viscous flow zone to a region approximately one blade radius surrounding the blade,

Figure 5 shows the radial variation of normal forces at these wind speeds. It is seen that the full Navier-Stokes simulation does a better job of predicting the normal forces at these higher wind speeds. The hybrid method does a fair job of predicting the overall trend, but overpredicts the loads and does not match the predicted loads as well as the Navier-Stokes simulations do.

The turbulence model was found to have little effect at these high wind speeds. In our simulations, we found that at these three wind speeds the flow separated close to the leading edge (where the boundary layer is thin and the mixing effects associated with eddy viscosity are small). At these high speeds, the flow field over most of the rotor was dominated by the separation near the leading edge, and showed little sensitivity of the flow field to the turbulence viscosity distribution downstream of the separation.

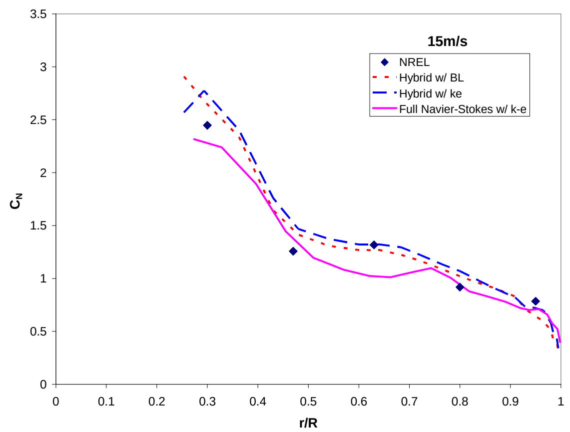

Figure 5a Comparison of Computed and Measured Radial Distribution of the Normal Force Coefficients for the 15 m/sec Case.

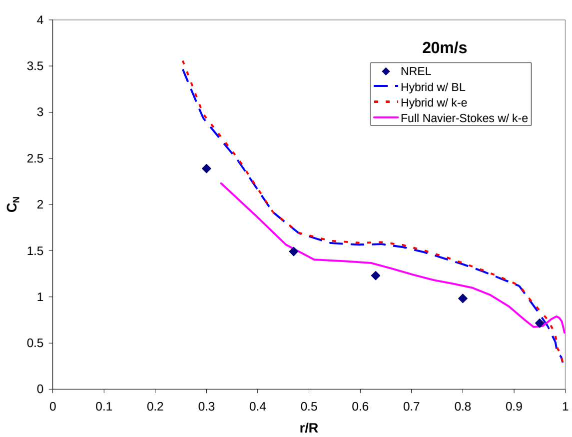

Figure 5b Comparison of Computed and Measured Radial Distribution of the Normal Force Coefficients for the 20 m/sec case

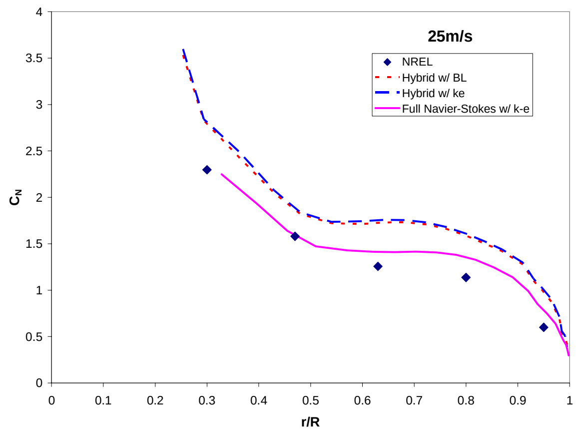

Figure 5c Comparison of Computed and Measured Radial Distribution of the Normal Force Coefficients for the 25m/sec case.

Figure 6 shows the tangential force variation along the radial direction at these wind speeds. This component is directed along the blade chord line. A positive value indicates that the force is directed towards the leading edge, while a negative value indicates that the force is directed towards the trailing edge.

At the 15 m/sec case, figure 6 indicates that the full Navier Stokes simulation does the best job of predicting the tangential force coefficient. The Navier-Stokes simulation captures the tip vortex and the associated inflow field from first-principles, while the hybrid method models the vortex using piecewise line segments, uses the Biot-Savart law to compute the inflow field. These two methods thus differ considerably in how the separated flow is predicted in the immediate vicinity of the blade tip. This had a more pronounced effect on the tangential forces than the normal forces discussed earlier, and caused the differences between the Navier-Stokes and the hybrid method near the tip.

At the higher wind speeds of 20 m/sec and 25 m/sec, all the three methods (Full Navier-Stokes, hybrid method with k-ε turbulence model, and hybrid method with Baldwin-Lomax turbulence model) did a reasonable of predicting the tangential forces except near the tip region. At these wind speeds, the tangential forces are dominated by pressure drag effects.

Figure 7 shows the surface pressure distributions at a typical speed of 20m/sec. The behavior at the other two wind speeds is similar. Because the present analysis is an unsteady time marching analysis and because the flow is unsteady at high wind speeds, these Cp plots are just a snapshot of the pressure field at an instance in time.

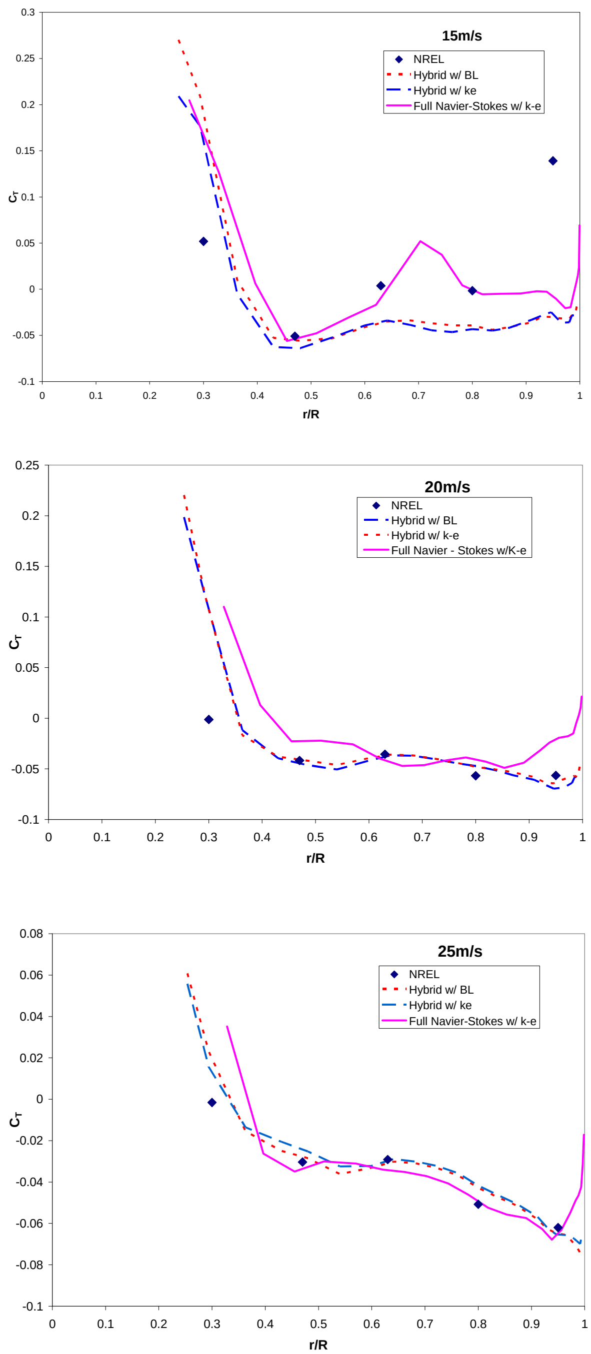

Figure 6 Comparison of Computed and Measured Radial Distribution of the Tangential Force Coefficients for the 15, 20, and25 m/sec cases

As in the case of integrated loads, our results indicated that the turbulence model had only a small effect on the predictions, presumably because the flow is separated very close to the leading edge at these high wind speeds. For clarity, we have not shown the Baldwin-Lomax model based results here.

From
simula
pressu
rotor,
metho
pressu
nearly
(predo
overes
under

At the
begin
Navie
with
stated
seen
with
It ma
comp

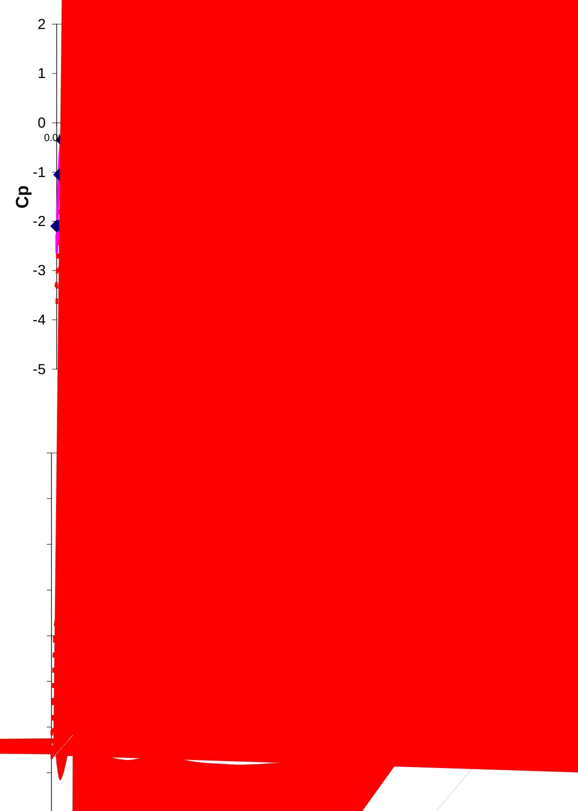

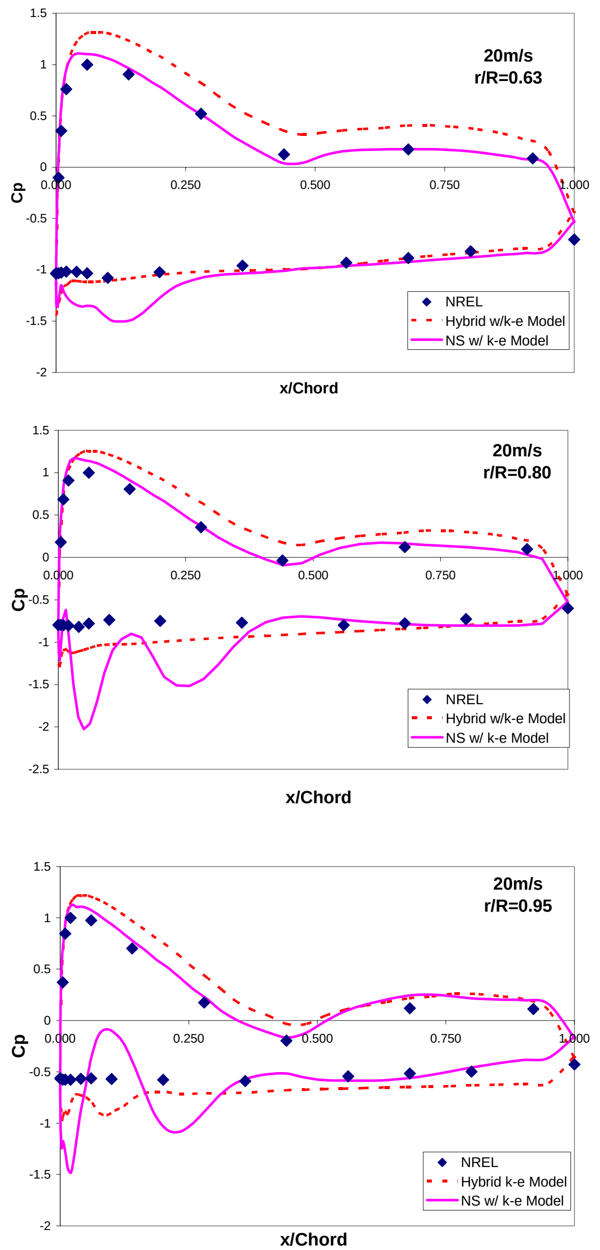

Figure7b. Computed and Measured C_P distribution at several radial locations for the 20 m/sec case

CONCLUDING REMARKS

A hybrid approach previously used to model HAWT aerodynamics at low wind speeds has been extended to higher wind speed conditions. Comparisons with a full Navier-Stokes simulation and experimental data have been made. Effects of turbulence model have been studied. The following conclusions may be drawn from the results obtained to date.

a) Among the two approaches, Navier-Stokes based solutions are clearly better than the hybrid method solutions in quality for all the properties studied: normal force distribution and tangential force distribution along the radial direction, and surface pressure distributions. The 40% increase in computer time for the Navier-Stokes equations relative to hybrid method may be a small price to pay in view of the better correlations with experiments.

b) The root vortex is very weak due to the low strength of the bound circulation in the inboard region. It has negligible effect on the overall solution, and may be neglected, while computing the induced velocity using Biot-Savart Law.

c) The k-ε model and the Baldwin-Lomax model based simulations both gave results that are very similar. At the high wind conditions considered here, the flow is extensively separated starting from the blade leading edge, and the use of low order models is not appropriate. It is therefore recommended that the k-ε model be used in these calculations. Evaluation of other 2-equation models that have been demonstrated by other researchers to do better in separated flows is also recommended.

d) None of the simulations presented here did a good job of predicting the tangential force coefficients in the immediate vicinity of the blade tip. At low wind speeds this force component is critical to accurately predicting the low speed torque. Calculations are underway at this writing, to determine if the behavior near the tip can be improved with the use of progressively fine grids.

REFERENCES

1. Tangler, J. L., Smith, B. and Jager, D.. “SERI Advanced Wind Turbine Blades”, NREL/TP-257-4492, Golden, CO, 1992.
2. Eppler, R.,*Airfoil Design and Data*, New York, NY, Springer-Verlag, 562 pp., 1990.
3. Selig, M. S., Donovan, J. F. and Fraser, D. B. *Airfoils at Low Speeds*, Soartech 8, Virginia Beach, VA, H. A. Stokely, 1989.
4. Glauert, H. “An Aerodynamic Theory of the Airscrew.” ARC R&M 786, January 1922.
5. Hansen, A. C. and Butterfield, C. P., "Aerodynamics of Horizontal-Axis Wind Turbines," *Annual Review of Fluid Mechanics.* Vol. 25, pp. 115-149, 1993.
6. Laino, D. and Butterfield, C. P., "Using YAWDYN to Model Turbines with Aerodynamic Control Systems," ASME Wind Energy Conference, New Orleans, LA, 1994.
7. Leishman, J. G. and Beddoes, T. S., "A semi-Empirical Model for Dynamic Stall," *Journal of*

the American Helicopter Society, Vol. 34, pp. 3-17, 1989.

8. Earl P. N. Duque, C. P. van Dam, and Shannon C. Hughes, "Navier-Stokes Simulations of The NREL Combined Experiment Phase II Rotor", AIAA-99-0037, January 1999.
9. Sorensen, N. N., and Michelsen, J. A., Aerodynamic predictions for the Unsteady Aerodynamics Experiment Phase II rotor at the National Renewable Energy Laboratory, AIAA 2000-0037.
10. Sørensen, N., Michelsen, J., and Schreck, S., "Navier-Stokes Predictions of the NREL Phase VI Rotor in the NASA Ames 80- by-120 Wind Tunnel", Wind Energy, Volume5, Number 2/3, April- September 2002.
11. Madsen, H., Sørensen, N., and Schreck, S., "Yaw Aerodynamics Analyzed with Three Codes In Comparison with Experiment", AIAA-2003-0519.
12. Duque, E., Burklund, M., and Johnson, W., "Navier-Stokes and Comprehensive Analysis Performance Predictions of the NREL Phase VI Experiment," AIAA-2003-0355.
13. Benjanirat, S., Sankar, L., and Xu, G., "Evaluation of Turbulence Models of the Prediction of Wind Turbine Aeordynamics", AIAA-2003-0517.
14. Xu, G., "Computational Studies of Horizontal Axis Wind Turbines", Doctoral Thesis, School of Aerospace Engineering, Georgia Institute of technology, Atlanta, GA.
15. Xu, G. and Sankar, L., "Application of a Viscous Flow Methodology to the NREL Phase VI Rotor", AIAA-2002-0030.
16. Xu, G., and Sankar, L., "Computational Study of Horizontal Axis Wind Turbines," Presented at AIAA Aerospace Science Meeting, Reno, Nevada, 1999, AIAA paper 99-0042.
17. Xu, G., and Sankar, L., "Effects of Transition, Turbulence and Yaw on the Performance of Horizontal Axis Wind Turbines," Presented at AIAA Aerospace Science Meeting, Reno, Nevada, 2000, AIAA-2000-0048.
18. Gorski, J., "A New Near-Wall Formulation for the k-epsilon Equations of Turbulence", AIAA 24th Aerospace Sciences Meeting. January 6-9, 1986/ Reno, Nevada.
19. Wu, Jiunn-Chi, Huff, D. and Sankar, L.N., "Evaluation of Three Turbulence Models in Static Airloads-and Dynamic Stall Predictions," Journal of Aircraft, Vol. 27, No. 4, April 1990, pp382-384.